

UNCLASSIFIED

Defense Technical Information Center  
Compilation Part Notice

ADP012156

TITLE: From Diamond to Carbon Nanotube Field Emitter

DISTRIBUTION: Approved for public release, distribution unlimited

This paper is part of the following report:

TITLE: Materials Research Society Symposium Proceedings. Volume 675.  
Nanotubes, Fullerenes, Nanostructured and Disordered Carbon. Symposium  
Held April 17-20, 2001, San Francisco, California, U.S.A.

To order the complete compilation report, use: ADA401251

The component part is provided here to allow users access to individually authored sections of proceedings, annals, symposia, etc. However, the component should be considered within the context of the overall compilation report and not as a stand-alone technical report.

The following component part numbers comprise the compilation report:

ADP012133 thru ADP012173

UNCLASSIFIED

## From Diamond to Carbon Nanotube Field Emitter

O. Gröning, L.-O. Nilsson, P. Gröning and L. Schlapbach

Gruppe für Festkörperphysik

Physik Departement der Universität Fribourg, Chemin du musée 3, CH-1700 Fribourg  
(Switzerland)

### Abstract

In this paper we review the physics and the expectations that were put into the negative electron affinity (NEA) mediated field emission of chemical vapor deposition CVD diamond films and how the emitter technology made possible by this mechanism could have challenged the classical metal micro-tip field emitter arrays. We discuss the dependency between emitter performance of micro-tip emitter arrays and feature size (size of the field enhancing tip) and due to this to the connection between emitter performance and fabrication costs.

We introduce the concept of the field enhancement distribution function  $f(\beta)$  for a useful characterization of the field emission properties of thin film emitter and show how this distribution function can be measured by scanning anode field emission microscopy. Using  $f(\beta)$  measured on a thin film of randomly oriented multiwalled carbon nanotubes we show that even these kinds of low cost emitters can show a field emission performance comparable to micro-tip arrays, yet that the large spread in field enhancement values between the individual emitter prevent this performance to be fully exploited. This because the field range in which such thin film emitters can be operated is limited due to emitter disruption and triggering of vacuum arcs. Simulations show how resistor-limited emission can solve these limitations.

### Introduction

In recent years various kinds of carbon thin films have been recognized as interesting materials for field emission cathodes. The development of the field emission flat panel display in the same time has further boosted this interest. Therefore investigation of the field emission properties and mechanisms of carbon based materials as single crystalline and chemical vapor deposition (CVD) diamond, diamond like carbon, nanocrystalline graphite and carbon nanotubes has become a domain of very active research. Though field electron emission from a perfectly flat metal surface requires electric field on the order of  $2500 \text{ V}\mu\text{m}^{-1}$ , for the carbon based materials mentioned above field emission currents could be observed for applied electric fields below  $10 \text{ V}\mu\text{m}^{-1}$ .

Classical Fowler-Nordheim like field emission describes the tunneling of electrons close to the Fermi energy through a narrow surface potential barrier. When an electric field of the order of  $2500 \text{ V}\mu\text{m}^{-1}$  is present at a typical metal surface with a work function of 5 eV the surface potential step confining the electrons to the solid, becomes a triangular shaped surface potential barrier. As the width of the barrier at the Fermi energy approaches 2 nm, the electrons have a non-negligible probability of tunneling from the solid into vacuum. Fields of the order of  $2500 \text{ V}\mu\text{m}^{-1}$  can practically only be created when the field enhancing effect of conducting tip-like structures is exploited. The field amplification of a tip at its apex is in first approximation equal to the aspect ratio (height/radius) of the tip.

Although the effects of thermionic and field electron emission were discovered at about the same time, thermionic emission is almost exclusively used for technical applications where free electrons in vacuum are required. The first reasons for this is that thermionic emitters are rather simple, in the simplest case it is just a heated tungsten or tantalum wire. Further they can reliably deliver high emission currents of up to  $400 \text{ Acm}^{-2}$  for many thousand hours[1]. Field emitters on the other hand are able to deliver very high emission current densities of the order of  $10^6 \text{ Acm}^{-2}$ , but as tip like structures are needed to created the electric field required for the emission, the actual emitting area, which is the apex of the field enhancing tip, is usually very small. The higher the field enhancement the smaller the emitting area gets so that the emission

current from a single field emission tip is usually small. Therefore field emitter found applications only where the high emission current density and the small emitting area, leading to a high brightness, are advantageous and where the total emission current has not to be very high such as in high resolution electron microscopy. Though thermionic emitter have numerous advantageous features for technological applications, they are not suited for miniaturization due to the high operation temperature of 950°C-2500°C. Miniaturization of thermionic emitter means to deal with increasing temperature gradients in the device. So that devices using thermionic emitter are difficult to build smaller than a few mm. Field emitter in contrast do not have such limitations, actually the miniaturization of field emitter is a key element to their success in vacuum microelectronics. The miniaturization of field emitters to micrometer sizes allows to integrate a large number of emitting tips on a surface and therefore achieving emission current densities with respect to the device surface which are comparable to emission current densities of thermionic emitter. A simple picture of such a field emitter is an array of micrometer sized tips on a flat surface.

### The metal micro-tip field emitter array

Using some basic assumptions it is possible to estimate the emission current density of such a field emitter array, where the current density is with respect to the surface of the device and not the actual emitting area of the tip apex. This definition of current density is useful for technological consideration, e.g. for the comparison of field emitter arrays with thermionic emitter.

As the basis of this estimation stands the description of the emission current of a single tip as a function of the electric field at the emission site. One has to distinguish between the applied field  $E_{apl}$  being the homogenous electric field perpendicular to the surface of the field emitter array and the local field  $E$  at the emission site (which is the tip apex). In a simple diode configuration of two parallel plates separated by a vacuum gap  $d$  the applied field would be given by  $E_{apl}=V/d$ , where  $V$  is the bias voltage between the plates and  $d$  being the separation of the plates. The local electric field at the apex of the  $i^{th}$  field emitter tip is then given by  $E_{apl} \cdot \beta_i$ , where  $\beta_i$  is the field enhancement factor of the  $i^{th}$  emitting tip. For our estimation of the emission current density we assume that all the tips are needle shaped (cylindrical shafts with spherical caps) having the same height  $h$  and the radius of curvature at the apex  $r$ . We have shown that for a tip array of identical tips the maximum emission current at a fixed applied field is obtained, when the spacing between the individual tip in the emitter array is twice their height  $h$ . An optimal emitter array would then be a hexagonal array of tips (height  $h$  and radius at the apex  $r$ ) where the next nearest neighbor distance is  $2 \cdot h$ . For this configuration the device surface area per tip  $A_{tip}$  and the emitting surface  $A_E$  are given by:

$$A_{Tip} = 2\sqrt{3}h^2 \quad (1) \quad A_E = \alpha\pi r^2 \quad (2)$$

where  $\alpha$  is a proportionality factor on the order of 1. So that the emission current density  $J_D$  with respect to the surface of the emitter array is given by:

$$J_D = \frac{A_E \cdot J_{FN}(E, \phi)}{A_{Tip}} = \frac{\alpha\pi}{2\sqrt{3}} \left(\frac{r}{h}\right)^2 J_{FN}(E, \phi) = 0.9 \left(\frac{1}{\beta}\right)^2 J_{FN}(E_{apl} \cdot \beta, \phi) \quad (3)$$

where  $J_{FN}$  denotes the Fowler-Nordheim relation giving the emission current density as a function of the local field  $E$  and the emitter work function  $\phi$ . The maximum current density  $J_D$  will depend on the maximum local current density  $J_{FN}$  which a tip can support. This value will be material dependent and will also depend on the requirements with regard to emitter life time. For a constant work function (given by the emitter material) and a given maximum local emission

current density  $J_{FN}$ , the value of  $E=E_{apli}*\beta$  can be determined from the Fowler-Nordheim relation. So that the maximum device emission current density  $J_D$  can be determined as a function of the applied field at which the device should deliver the maximum current density  $J_{FN,max}$ . Figure 1 displays the dependence of the maximum device emission current density  $J_D$  and the applied field of operation for different maximum local emission current densities  $J_{FN}$ . As one can observe in order to achieve a  $J_D$  of the order of  $10 \text{ Acm}^{-2}$  (which is a typical current density of thermionic emitter) in an applied field range of  $2\text{-}10 \text{ V}\mu\text{m}^{-1}$  requires that the single emitters can sustain local field emission current densities in the range of  $10^6\text{-}10^8 \text{ Acm}^{-2}$ .

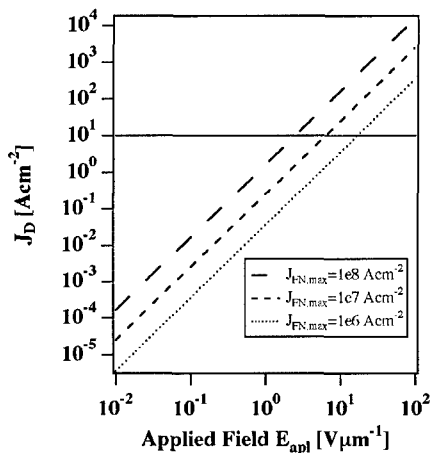


Figure 1

Emission current density with respect to the emitter array surface area  $J_D$  as a function of the applied field of operation. The dashed curves represent the maximum theoretical  $J_D$  for a hexagonal field emitter array for different max. Emission current densities per single emitter  $J_{FN,max}$ .  $E_{apli}$  denotes the field needed to achieve the max. single emitter current density  $J_{FN,max}$ .

Using high density, gated metal micro tip field emitter arrays, values of  $J_D$  of  $100 \text{ Acm}^{-2}$  can be achieved at applied fields of the order of  $100 \text{ V}\mu\text{m}^{-1}$ [2]. With a  $J_D$  of the order of  $100 \text{ Acm}^{-2}$  such field emitter array can challenge thermionic emitter. However the production of metal micro tip field emitter arrays involves expensive lithographic processes, which has triggered the interest in efficient low cost field emitting materials.

One of the disadvantage of using field emitter for large area electron sources is the need to fabricate a large number ( $\sim 10^6\text{-}10^8 \text{ cm}^{-2}$ ) of micrometer or even sub micrometer sized tips. Due to the steep current-field characteristic of field emission the requirement to the geometric properties of the individual tips is very high further complicating the manufacturing process and raising production costs. For a work function of 5 eV the relative change  $dI/I$  of emission current of a single emitter is a factor of ten with a relative change of field enhancement  $d\beta/\beta$  of 10%. Which means that if the aspect ratio and therefore the field enhancement of the field enhancing tip in a field emitter array is controlled within 10%, the field emission current from the individual tips will show a scatter over one order of magnitude.

The key to success of field emission tip arrays is to produce micrometer sized tips with a high density and with a high degree of control over the aspect ration of the individual tip. The fabrication techniques employed in the semiconductor industry offer the possibilities to fabricate such emitter arrays. As the Moore's law, describing the exponential decrease of feature size in semiconductor industry with time, one can expect a similar development for field emitter arrays. Here the decrease in feature size and therefore an increase in emitter density will increase the performance of the emitter array. Unfortunately there is a second Moore's law stating that the exponential decrease in feature size comes with an exponential increase of production costs and wherefore in analogy, the fabrication of micrometer sized emitter arrays is expensive.

## Chemical vapor deposition diamond field emitter

CVD diamond films seemed to offer a field emitter which had not to rely on field enhancing structures and therefore not being subjected to the unfavorable relation of emitter performance and emitter cost of the field emission tip arrays. Because of the negative electron affinity (NEA) of the hydrogen terminated diamond surface it was thought that diamond could deliver electron emission at moderate local electric fields of the order of  $10 \text{ V}\mu\text{m}^{-1}$  and without the need of field enhancing structures[3]. These expectations were backed by numerous experimental observations of field emission at applied fields below  $20 \text{ V}\mu\text{m}^{-1}$ [4].

In a semiconductor the electron affinity is defined as the energy difference between the vacuum level (lowest electron state in vacuum) and the conduction band minimum. Usually in ordinary semiconductors such as silicon or germanium this energy difference is positive. When the work function of the semiconductor is comparable to the gap energy, as in the case of diamond, the electron affinity can become negative. This means that an electron in the conduction band can be emitted into vacuum without experiencing a surface potential barrier. This effect can be readily observed in photo- or secondary emission experiments on NEA single crystalline or CVD diamond.

A CVD diamond field emitter making use of NEA would therefore rely on three main processes:

- Injection of electrons into the conduction band of a CVD diamond thin film at the diamond-metal interface.
- Transport of the electrons in the conduction band to the diamond surface.
- Emission of the electrons into vacuum due to NEA.

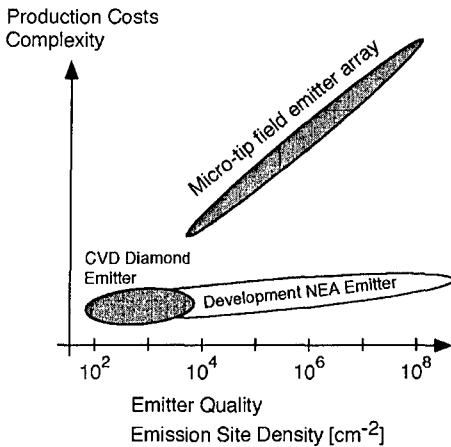


Figure 2

The diagram illustrates qualitatively the dependence between the emitter quality expressed by the emission site density and the production costs.

The way to an efficient NEA CVD diamond emitter would mean to optimize each of the three above mentioned points. The injection would require a very narrow Schottky barrier and an effective field penetration into the diamond film. The transport of the electrons to the surface requires a low defect density and a low density of grain boundaries in order to prevent trapping and recombination of electrons, which would then be lost for the emission. The emission at the diamond surface requires that the entire surface is in the NEA state, which can be controlled by the surface hydrogen termination and by the crystalline faceting of the surface.

The optimization of a NEA CVD diamond field emitter would proceed via the control of interface, bulk and surface properties of the diamond thin film. These are typical tasks in thin film deposition and can be achieved without considerably increasing the costs of the deposition process. The key point making the concept of diamond NEA emitter so attractive, is that this emitter is not submitted to the close relation between emitter performance and emitter costs as the field emission tip arrays.

Due to the second Moore's law of semiconductor industry the field emission tip arrays have to battle against the relation between feature size and production costs. Meaning that a decrease in feature size (size of the tip), giving an increased emitter density and therefore increased emitter performance, is connected with an considerable increase in the production costs. In Fig. 2 the emitter quality is expressed as the emission site (or emitter site) density on the horizontal axis. The vertical axis expresses qualitatively the production costs, where the scale would be rather logarithmic than linear.

Although the experimentally observed field emission properties of CVD diamond films, with emission site densities ranging from a few tens to  $10^3$  per  $\text{cm}^2$  (dark gray ellipse), can not match the micro-tip field emitter arrays, CVD diamond thin films seemed to offer a great potential for the further development. Assuming the NEA emission mechanism, CVD diamond thin films could be developed to show emission from the hole cathode area and not from the relatively small surface area of a tip apex. The emission current density would only be limited by the injection current density at the metal-diamond interface.

The actual development in CVD diamond field emitter cathodes could not back this exciting perspective. The improvements made in the CVD diamond film emitter was just opposite to what NEA emission would require. Figure 3 shows the emission image on a phosphorus screen of a nanocrystalline CVD diamond film at different applied electric fields.

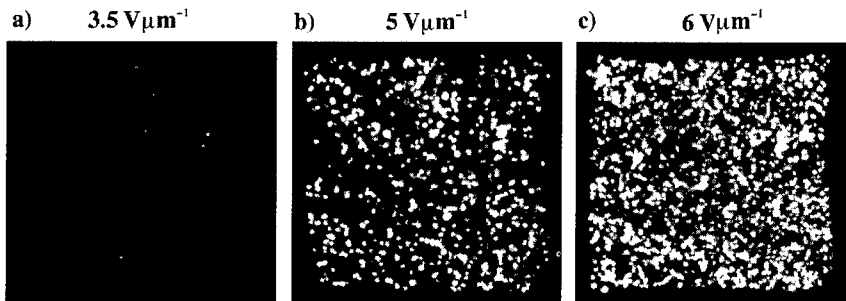


Figure 3

Field emission image on a phosphorus screen of a nanocrystalline CVD diamond film of  $10 \times 10 \text{ mm}^2$  at different applied fields.

Whereas the NEA emission mechanism would require high crystalline quality (as discussed above) the diamond films showing good field emission properties such as displayed in Fig. 3 are of nanocrystalline and highly defective nature. Further where NEA emission required insulative films for field penetration the nanocrystalline CVD diamond films are in general rather conductive. Also the influence of the contact-diamond interface to the field emission properties has shown not to be as essential as expected from NEA emission.

As can be seen from Fig. 3 the emission is spotty, where the spot density (emission site density) is a function of the applied field. The difficulty in the investigation of the field emission properties of these kind of thin films emitters resides to a good deal in the spotty nature of the emission. This because the field emission I-V measurements can not give conclusive information



in large numbers using low cost deposition techniques. The emission of carbon nanotubes is clearly governed by their high aspect ratio and therefore by their field enhancement.

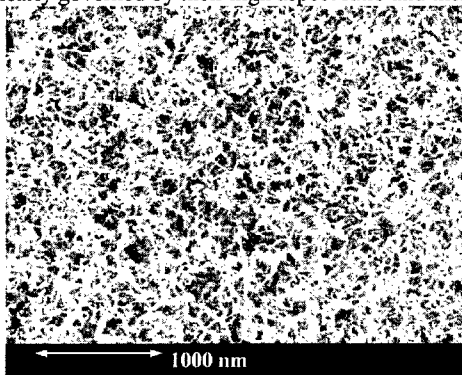


Figure 5

SEM micrograph of a randomly oriented MWNT thin film deposited on a silicon wafer.

Figure 5 displays a film of randomly oriented MWNT grown on a silicon wafer by pyrolysis of acetylene in a nitrogen atmosphere at substrate temperatures of 900° C. As catalyst for the nanotube growth 10 nm Ni was sputtered on the silicon. Such kind of randomly oriented nanotube thin films with a rather low density of tubes show already a very good field emission performance.

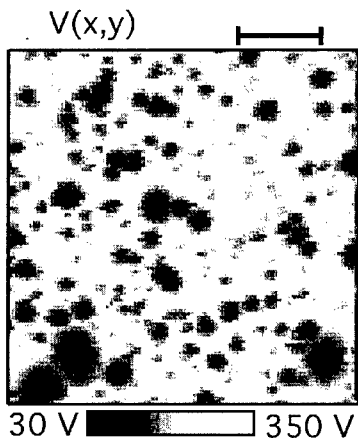


Figure 6

Scanning anode field emission measurement of a MWNT thin film (sample displayed in Fig. 5). The map shows the extraction voltage as function of the x-y anode position for a constant emission current of 10 nA and an anode-sample distance of 5 μm. The scale bar is 50 μm.

Figure 6 displays a scanning anode voltage map  $V(x,y)$  of the nanotube thin film of Fig. 5 showing the voltage needed to obtain a fixed emission current of 10 nA as a function of the position of the anode. In this measurement the surface of the nanotube thin films is scanned at a constant distance of 5 μm by a tip anode of 1 μm tip radius. The resulting voltage map  $V(x,y)$  is displayed as gray scale image plot. The individual emission sites show up as dark spots in this plots indicating that a low voltage is needed at this positions to obtain the fixed emission current of 10 nA. Strong emission sites are characterized by a low value of the anode voltage at the

minimum of the emission spot and also by the size of the emission spot. As one can see there is a large scatter in the field emission performance of the individual emitters. In the scanned area of  $200 \times 200 \mu\text{m}^2$  157 emission sites can be identified which corresponds to a density of about  $400'000 \text{ cm}^{-2}$ . It becomes clear from Fig. 6 that the characterization of the emission properties of a nanotube thin film emitter means the characterization of a large ensemble of individual emitter with different emission properties.

In order to obtain a realistic description of the electron emission from a thin film emitter ensemble, the emission properties of a single site need to be characterized. To do so we start the assumption that the FN-law correctly describes the current-field characteristics of MWNT field emitter. For our considerations we use the simplified formula of Brodie and Spindt [7]:

$$I = A \cdot \frac{1.5 \cdot 10^6}{\phi} E_{\text{Apl}}^2 \beta^2 \exp\left(\frac{10.4}{\sqrt{\phi}}\right) \exp\left(\frac{-6.44 \cdot 10^7 \phi^{1.5}}{E_{\text{Apl}} \cdot \beta}\right) \quad (1)$$

$I$  is the emission current of a single emitter in Ampere,  $\phi$  the emitter work function in eV,  $\beta$  the field enhancement factor and  $E_{\text{Apl}}$  the applied electric field.  $E_{\text{Apl}}$  is given by the applied voltage  $V$  and the anode-cathode separation  $d$  by  $E_{\text{Apl}} = V/d$ . The product of  $\beta$  and  $E_{\text{Apl}}$  gives the local electric field present at the emission site  $E_{\text{Site}} = E_{\text{Apl}} \cdot \beta$ . Changes in the emission current of different emitter according to (1) arise from changes of the emitting surface  $A$ , the work function  $\phi$  and of the field enhancement factor  $\beta$ . Using FES we have determined the work function of MWNT emitter to be  $4.9 \pm 0.2$  eV and from this value also the emitting surface could be determined to range from  $10^{-8}$  to  $10^{-10} \text{ cm}^2$  [8]. One has to be aware that although  $A$  has the dimensions of a surface it also contains information about the electronic structure of the emitter and therefore doesn't only account for the geometric emitting surface.

If we assume that all the MWNT emitter have the same work function  $\phi = 4.9$  eV and the same emitting area  $A = 10^{-9} \text{ cm}^2$  relation (1) becomes very simple:

$$I = 3.4 \cdot 10^{-14} E_{\text{Apl}}^2 \cdot \beta^2 \exp\left(\frac{-7 \cdot 10^8}{E_{\text{Apl}} \cdot \beta}\right) \quad (2)$$

Leaving the field enhancement  $\beta$  the only parameter determining the emission properties of a single emitter. To characterize the emission properties of a large ensemble of emitter such as the nanotube thin film of Fig. 5 and Fig. 6 we just need to know the field enhancement distribution function  $f(\beta)$  [9]. Where  $\Delta N = f(\beta) \Delta \beta$  is the number of emission sites per unit area having a field enhancement factor in the interval  $[\beta, \beta + \Delta \beta]$ . The determination of this field enhancement distribution function  $f(\beta)$  characterizes the thin film field emission properties. Of course the question has to arise whether the assumption of a constant work function (justified by the fact that all emitter are of the same material) and a constant emitting surface (justified by the fact that all emitter are of the same dimensions) is not to severe. In fact one can test how a relative change of  $\phi$  and  $A$  in relation (1) influences the value of  $\beta$  in order to obtain a constant emission current. For an emission current of 10 nA a relative change of the work function of 0.2 eV  $\Rightarrow \Delta \phi / \phi = 0.2 / 4.9 = 0.04$  would lead to a relative change of the field enhancement factor of only 5% ( $\Delta \beta / \beta = 0.05$ ). Under the same conditions a relative change of the emitting surface of one order of magnitude  $\Delta A / A = 10$  leads to a relative change of only 11% for  $\beta$  ( $\Delta \beta / \beta = 0.11$ ).

From voltage maps such as displayed in Fig. 6 the  $f(\beta)$  can be determined. As the voltage scan is performed at a constant emission current, according to relation (2) the local value of  $E_{\text{Site}} = E_{\text{Apl}} \cdot \beta(x, y) = V(x, y) \cdot \beta(x, y) / d$  is constant too. Here  $E_{\text{Site}}$  denotes the local electric field present at the emission site needed to obtain the fixed emission current of the voltage map. The local field enhancement  $\beta(x, y)$  map can therefore be derived from the voltage map  $V(x, y)$  by  $\beta(x, y) = E_{\text{Site}} \cdot d / V(x, y)$ .

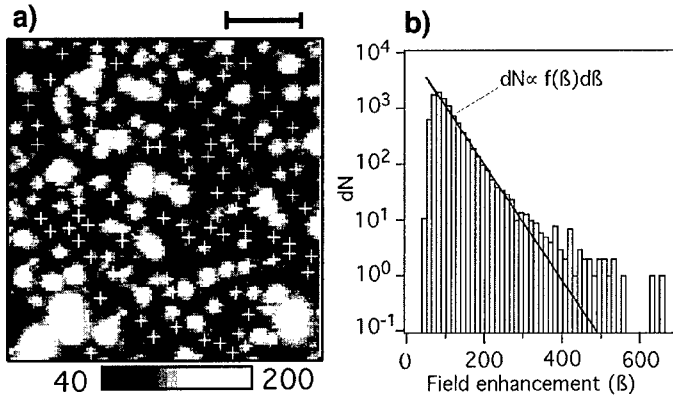


Figure 7

Diagram a) displays the field enhancement map derived from the voltage map of Fig 6. The scale bar is 50  $\mu\text{m}$  and the white crosses denote the emitter positions. Diagram b) shows the histogram of the field enhancement map from which the field enhancement distribution function can be derived.

Figure 7a displays the field enhancement map  $\beta(x,y)$  derived from the voltage map of Fig. 6. The emission sites now show up as local spots of high field enhancement values. The histogram of the beta map (see Fig. 7b) is now proportional to the field enhancement distribution function  $f(\beta)$ . Where the proportionality  $\alpha$  factor equals:

$$f(\beta) = \alpha \cdot \text{Hist}(\beta(x,y), \Delta\beta) \qquad \alpha = \frac{N_{\text{emitter}}}{N_{\text{pixels}} \cdot \Delta\beta \cdot A}$$

Where  $N_{\text{emitter}}$  is the number of emission sites in the  $\beta$ -map (157 in this case),  $N_{\text{pixel}}$  is the number of measurement points in the  $\beta$ -map ( $100 \cdot 100$  in this case),  $\Delta\beta$  is the bin width of the histogram and  $A$  is the surface area of the  $\beta$ -map ( $4 \cdot 10^{-4} \text{ cm}^2$ ). As can be seen from Fig. 7b  $f(\beta)$  has the shape of an exponentially decreasing function with  $\beta$ . The histogram over estimates  $f(\beta)$  in the high  $\beta$  region due to the larger apparent size of high  $\beta$  emission sites in the  $\beta$ -map. From Fig. 7b one can determine the field enhancement distribution function for this sample to be:  $f(\beta) = 1.2e5 \exp(-0.024 \cdot \beta) [\text{cm}^{-2}]$ .

From the voltage map of Fig. 6 one can determine that there are about 400'000 emitter per  $\text{cm}^2$  delivering emission currents of 10 nA for applied fields below  $40 \text{ V}\mu\text{m}^{-1}$ . Compared with metal microtip arrays operating at applied fields around  $100 \text{ V}\mu\text{m}^{-1}$  this figure seems very promising. The constant current measurement however is particular because a field emission cathode will be operated in most of the cases at a constant applied field. Under such condition the large spread of field enhancement values (see Fig. 7b) will lead to the situation that under constant field conditions the emission current will be carried only by a few, high  $\beta$  emission sites.

Figure 8 shows simulations of the emission image on a phosphorus screen (comparable to the measurements of Fig. 3 for  $f(\beta) = 1.2e5 \exp(-0.024 \cdot \beta) [\text{cm}^{-2}]$  assuming relation (2) for the emission current of a single emitter. Figure 8a displays the emission image for an applied field of  $4.4 \text{ V}\mu\text{m}^{-1}$  giving an emission current density of  $0.31 \text{ mAcm}^{-2}$ .

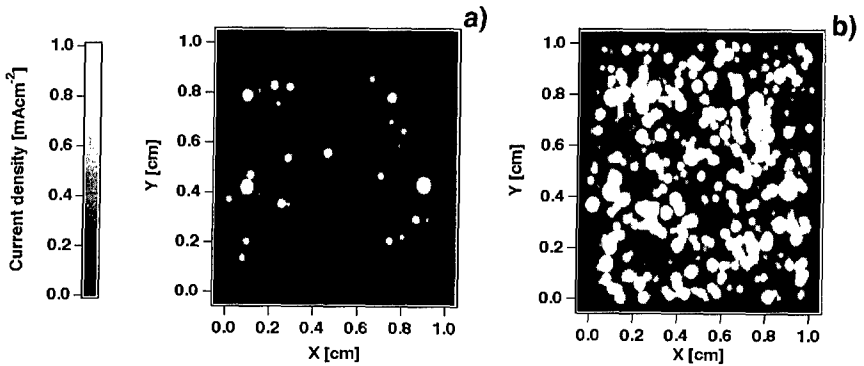


Figure 8

Diagram a) and b) display field emission simulations of a field enhancement distribution function  $f(\beta) = 1.2e \exp(-0.024 * \beta)$  [ $\text{cm}^{-2}$ ] at applied field of  $4.4 \text{ V}\mu\text{m}^{-1}$  for a) and  $5.6 \text{ V}\mu\text{m}^{-1}$  for b). The emission site are randomly distributed.

As one can see the current is carried only by a few emitter and that there are a large intensity differences between the emitter. When the applied field is increased to  $5.6 \text{ V}\mu\text{m}^{-1}$  the emission current density has increased to  $16.7 \text{ mAcm}^{-2}$ . The increase in field has increased the emission site density as new emitter with lower  $\beta$  become visible, at the same time the high  $\beta$  emitter are now delivering such high emission currents that the screen is by far in saturation and that these emitter start to disrupt, burn-out or even trigger vacuum arcs. This means that for such emitting films the emission site density on the screen is not limited by the actual emitter density which as we have seen can be very high, but by the applied field level at which irreversible damage to the thin film occurs by emitter disruption or vacuum arcing.

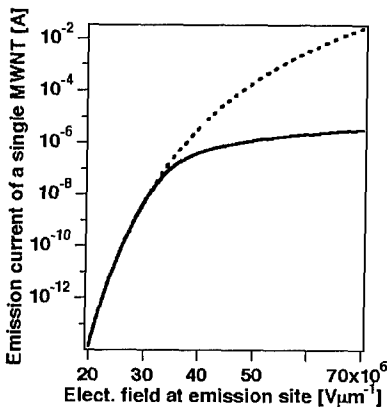


Figure 9

The diagram shows the current-field characteristics for a single MWNT emitter according to relation (2) (dashed line) and the according parallel resistor limited characteristic (solid line).

The introduction of a current limitation in the emission characteristic, e.g. by a parallel resistor for each emission site can improve this problem considerably. Figure 9 displays the current-field characteristic for a resistor limited emission (solid line) derived from relation (2) (dashed line). The resistor value has been chosen to limit the emission current of a single emission site at about  $1 \mu\text{A}$ . If we now take the current limited emission characteristic for the

simulation of the emission behavior for the same  $f(\beta)$  as for Fig. 8 one can observe how the emission homogeneity is considerably increased at the expense of a higher field of operation.

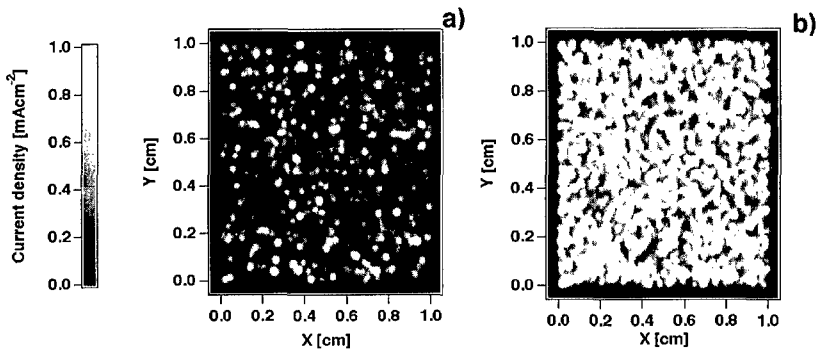


Figure 10

Simulation of the emission analog to Fig. 8 for resistor limited emission at  $5.6 \text{ V}\mu\text{m}^{-1}$  a) and  $6.9 \text{ V}\mu\text{m}^{-1}$  b).

Figure 10a displays the simulation of the emission image for the resistor current limited characteristic of Fig. 9 analog to the simulations of Fig. 7. One can see that for an applied field of  $5.6 \text{ V}\mu\text{m}^{-1}$  the emission density is comparable to the analog simulation for the unlimited emission characteristics of Fig. 7b. But due to the current limitation the emission current density is only  $0.2 \text{ mAcm}^{-2}$  as compared to  $16.7 \text{ mAcm}^{-2}$  without current limitation. There are no emission sites reaching emission current levels critical for emitter disruption or arcing, that is why the applied field can be further increased. The emission current density is  $1.2 \text{ mAcm}^{-2}$  for an applied field of  $6.9 \text{ V}\mu\text{m}^{-1}$  in Fig. 10b. One can see that for a much lower emission current density the emission homogeneity is very much increased and the problem of emitter disruption and vacuum arcing can be solved by the current limitation.

## Conclusions

The attractivity of CVD diamond emitter as material for field emission cathodes had its origin in the possibility of this material to solve a major problem in the development of classical metal micro-tip field emitter arrays. The performance of a micro-tip emitter is connected to the feature size (and therefore tip density), so that better performance is linked with decreasing feature size. The problem arises from the fact the fabrication costs rapidly increase with decreasing feature size. Due to the NEA electron affinity of diamond it was thought that an emitter technology could be realized which does not depend on feature size, but on bulk, interface and surface properties of a thin film. Properties which can be controlled in the deposition process of the film and therefore development and optimization of the emitter is not necessarily connected with an increase in production costs. Today however it becomes more and more clear that the field emission of CVD diamond is also due to field enhancement at local structures and that therefore CVD diamond emitter are also subjected to the problematic relation between feature size and emitter quality. This of course, reduces the attractivity and the potential of this material for field emission applications considerably.

Carbon nanotube thin field emitter started from a similar situation as the CVD diamonds, in the sense that there is a low cost approach to fabricate thin film field emission cathodes. The difference to CVD diamond is that one agrees that the emission is due to field enhancement at small tips. We have showed that even for randomly grown MWNT thin films the emission site

density in a interesting applied field range of  $50 \text{ V}\mu\text{m}^{-1}$  the emitter density can surpass  $10^6 \text{ cm}^{-2}$  and is therefore comparable to micro-tip arrays, at a fraction of the production costs. Yet the exponential field enhancement distribution of such nanotube thin film emitter exhibit is an obstacle for reaching a high emission site density as the emission current will be carried by only a few emission sites. An increase in the applied field above some critical value will further lead to irreversible damage to the emitting film due to emitter disruption and triggering of vacuum arcs. This effect leads to the situation that the emitting film can not be operated in a field range where a high emission site density can be achieved. The introduction of a current limiting mechanism, e.g. parallel resistor for each emitter, can solve this problem. As can be seen from Fig. 5 a resistive layer between the nanotube film and the substrate does not work, because the nanotube form an interconnected conducting network. The situation changes when the nanotubes are grown in small patches electrically disconnected of about  $1 \times 1 \mu\text{m}^2$  which is easily achieved by patterning the growth catalyst[10]. The resistive layer would therefore limit the emission current of a single patch, where it has to be expected that there will be only one dominating emitter in each patch. The emission site density is the given by the patch density, which can be easily of the order of  $10^7 \text{ cm}^{-2}$ . This would be a low cost approach for the fabrication of a thin film field emitter, which can compete against the micro-tip arrays.

In general the fabrication cost will be a key issue in the success of nanotube field emitter and therefore in the optimization of nanotube field emission cathodes one has to find the balance between improvement of the emission properties and increase in process complexity and therefore fabrication costs.

## References

- [1] G. Gärtner, P. Geittner, H. Lydtin, A. Ritz, Appl. Surf. Sci. 111 (1997) 11
- [2] D. Temple, Materials Science and Engineering, R24 (1999) 185
- [3] M.W. Geis, J.C. Twichell, T.M. Lyszczarz, J. Vac. Sci. Technol. B14 (1996) 2060
- [4] C. Wang, A. Garcia, D.C. Ingram, M. Lake, M.E. Kordesch, Electron. Lett. 27 (1991) 1459
- [5] O. Gröning, O.M. Küttel, P. Gröning, L. Schlapbach, J. Vac. Sci. Technol. B17 (1999) 1970
- [6] O. Gröning, O.M. Küttel, P. Gröning, L. Schlapbach, J. Vac. Sci. Technol. B17 (1999) 1064
- [7] I. Brodie, C. Spindt, Advances in Electronics and Electron Physics 83 (1992) 1
- [8] O.Gröning, O.M. Küttel, Ch. Emmenegger, P. Gröning, L. Schlapbach, J. Vac. Sci. Technol. B18 (2000) 665
- [9] L. Nilsson, O. Gröning, P. Gröning, O.M. Küttel, L. Schlapbach, J. Appl. Phys. in press (2001)
- [10] L. Nilsson, O. Gröning, Ch. Emmenegger, O.M. Küttel, E. Schaller, L. Schlapbach, H. Kind, J.-M. Bonard, K. Kern, Appl. Phys. Lett. 76 (1999) 2071